

Design of ITSM-conditioned FBMC By Embedding Side-Information for Reduction of PAPR

B. PRAVALIKA*

R. GURUNADHA**

*Department of systems and signal processing, JNTU-K University College of Engineering, Vizianagaram, Andhra Pradesh, India.

**Department of Electronics and Communication Engineering, JNTUK-University College of Engineering, Vizianagaram, Andhra Pradesh, India.

Abstract:

The filter bank multicarrier utilizing balance quadrature amplitude modulation (FBMC/OQAM) is an up-and-comer transmission conspire for 5G remote correspondence frameworks. In any case, it has a high peak-to-average power ratio (PAPR). Because of the idea of covered sign structure of FBMC/OQAM, traditional PAPR decrease plans can't work adequately. As a particular answer for this, we expand the possibility of DFT spreading-based low top to average force proportion (PAPR). In this the PAPR is decrease is done hardly. In this paper, to additional improve the measure of PAPR decrease, we create the four applicant adaptations of the DFT-spread and Identically-Time-Shifted-Multicarrier (ITSM) moulded FBMC waveform and select the one with least pinnacle power. Subsequently, with a partial unpredictability overhead contrasted with the past DFT-spread FBMC, the proposed plot accomplishes a PAPR decrease tantamount to that of SCFDMA. Further, we insert the SI in the deliberate stage turn of the star grouping without extra energy or data transmission. The phase rotation varies as indicated by the SI and is basic to all information images in every LP-FBMC subframe. Ordinary FBMC and SI-FBMC results are thought about and SI-FBMC has low PAPR. The correlation of results is indicated utilizing recreated results acted in MATLAB.

Keywords

FBMC, QOAM, LP-FBMC, SI-FBMC, PAPR

1. Introduction

FBMC with OQAM is a multicarrier tweak conspire which depends on heartbeats with great time recurrence limitation property [1]. From here on, we will utilize FBMC to signify "FBMC/OQAM", in spite of the fact that there exist other FBMC variations as well. Contrasted with traditional orthogonal frequency division multiplexing (OFDM) utilizing cyclic prefix (CP) and rectangular heartbeats, FBMC has higher ghostly effectiveness as it can work without the need of a CP even with a recurrence specific channel. Additionally, it brings about much lower out-of-band power emanation inferable from the tight range regulation of FBMC beats just as generally solid flexibility to transporter recurrence balances and Doppler spreads [2]. These preferences give FBMC an extraordinary potential for the help of an assorted scope of present day utilize situations where adaptable time recurrence distributions are profoundly requested. While late headway of 3GPP shows that (windowed or sifted) OFDM will be utilized in 5G [largely for the

retrogressive similarity with inheritance Long Term Evolution (LTE) systems], the voice for embracing FBMC in future versatile organizations doesn't appear to decrease [3].

An essential element that recognizes FBMC from regular OFDM is that symmetry among various subcarrier waveforms holds in the genuine field as it were. This outcomes in the natural fanciful obstruction which should be deliberately managed particularly at the channel assessment stage, where channel coefficients should be assessed in the mind-boggling area. Broad examination endeavours have been made to moderate or beat this issue in FBMC frameworks, including both preface and dissipated pilot-based methodologies [2]. This paper is worried about the introduction-based channel assessment approach. Notable models incorporate pairs of pilots (POP) [4], interference approximation method strategy (IAM) [4]-[6], and interference cancellation method (ICM) [7]. Kofidisetal. present a complete review in [8] of this theme, including prelude plan

and related assessment techniques for FBMC frameworks furnished with numerous radio wires. The prelude PAPRs of these strategies, be that as it may, are generally neglected in the plan method. As of late, two kinds of low-PAPR prefaces have been accounted for in [9] and [10]. In any case, no expository proof has been given, just mathematical outcomes. At the point when a nonlinear force speaker model is thought of, [11] brings up that the IAM-R and IAM-C preambles1 experience the ill effects of helpless blunder rate execution because of their high PAPRs. It should be noticed that low-PAPR FBMC introductions are urgent in guaranteeing a down to earth framework execution. A high-PAPR prelude will in general drive the send power enhancer to its nonlinear area, which thus brings about a misshaped introduction signal (and consequently wrong gauges of channel coefficients). To keep away from this, specific force chills out might be applied however this could extensively lessen the viable preface power (again prompting channel assessment execution disintegration). With regards to OFDM, a decent answer for without SI-PAPR decrease is single carrier-frequency division multiple access (SC-FDMA) or single-carrier with frequency-domain equalization (SC-FDE). In SC-FDMA, only discrete Fourier transform (DFT) spreading is performed preceding the OFDM

2. FBMC OQAM System

In Figure 4.1, we can see the square graph of transmitter in FBMC/OQAM systems, where N means the quantity of subcarriers and $a_{m,n}$ is the n -th subcarrier of m -th QAM image. The information is handled with OQAM adjustment, where $A_m = [a_{m,1}, a_{m,2}, \dots, a_{m,N-1}, a_{m,N}]$ After sequential to resemble activity, the genuine and non-existent pieces of every image are communicated to subcarriers, separately Then, after the model sifting and stage balance, the FBMC/OQAM transmission information square can be got by superimposing all the subcarrier signals. The m -th time-space FBMC/OQAM information block signal is given underneath

adjustment. SC-FDMA accomplishes an essentially lower PAPR contrasted with OFDM while acquiring the benefits of OFDM over different waveforms. The equal with regards to FBMCs compares to DFT-spread FBMCs [13–16]. Among these plans, the Pruned DFT-Spread FBMC [13] has a similar PAPR as SC-FDMA yet higher OOB emanation than the traditional FBMC. Furthermore, if the quantity of apportioned subcarriers is little, a recurrence cyclic prefix (CP) is expected to stifle the between image obstruction.

Another sort of straightforward DFT-spread FBMC called Low PAPR FBMC (LP-FBMC) was proposed [14]. LP-FBMC accomplishes low PAPR tantamount to that of SC-FDMA, while acquiring all the benefits of FBMC, for example, its brilliant OOB concealment ability and no requirement for CP. Nonetheless, in contrast to SC-FDMA, worthless SI should be sent alongside each subframe. Albeit no-account SI per subframe is small, sending and accepting it is unquestionably a weight in framework plan. In this perspective, LP-FBMC is less alluring than SC-FDMA. Subsequently, on the off chance that we can adjust LP-FBMC to eliminate the SI trouble, at that point the changed LP-FBMC could be a more complete and serious answer for the PAPR issue in FBMC like SC-FDMA with regards to OFDM.

$$\begin{aligned}
 s_m(t) &= \sum_{n=1}^N a_{m,n} h_{m,n}(t) \\
 &= \sum_{n=1}^N \left\{ \Re\{a_{m,n}\} h(t - mT) + j \Im\{a_{m,n}\} h\left(t - mT - \frac{T}{2}\right) \right\} e^{j\phi_{m,n}} \\
 &\quad mT \leq t < (m + \beta + \frac{1}{2})T
 \end{aligned} \tag{1}$$

where $\Re\{.\}$ denotes the real part of $a_{m,n}$ and $\Im\{.\}$ denotes the imaginary part of $a_{m,n}$. T is the symbol period, β is the overlapping factor, and the response of the prototype filter is $h(t)$, and $\phi_{m,n} = n\left(\frac{2\pi t}{T} + \frac{\pi}{2}\right)$ represents an additional phase term. $s_m(t)$ is a single FBMC/OQAM data block signal formula. After adding all transmitted subcarrier signals, the time-domain signal $s(t)$ of consecutive data blocks is given as:

$$s(t) = \sum_{m=1}^M s_m(t), 0 \leq t \leq (M + \beta - 1/2)T - 1$$

(2) where M is the number of data blocks.

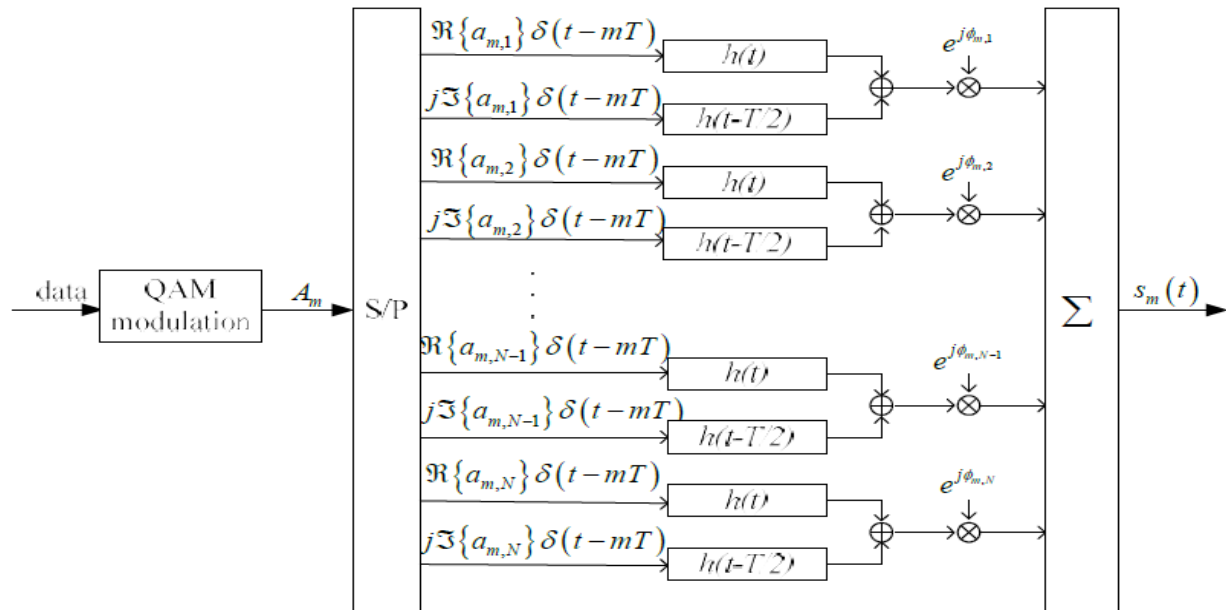


Fig 1. Block diagram of transmitter in FBMC-OQAM system

PAPR for FBMC/OQAM

In an ordinary OFDM framework, the length of an OFDM image is T. Thusly, there is no cover between adjoining image blocks, and a meaning of PAPR is proposed for every individual OFDM image. The meaning of PAPR is changed by the covered sign structure. s(t) is isolated into M+ b stretches, every one of which is equivalent to T (the last one is T/2). As needs be, the PAPR of every stretch is given as:

$$PAPR(dB) = 10 \log_{10} \frac{\max_{iT \leq t \leq (i+1)T} |s(t)|^2}{E[|s(t)|^2]}$$

(3)

Where $i = 0, 1, \dots, M + \beta - 1$ and $E[|S(t)|^2]$ is the s(t) expectation.

3. LP-FBMC

A. FBMC and DFT Spread FBMC

All through this task, we utilize the accompanying documentations: \Re = real part of x, \Im =imaginary part of x and Fig. 2(a) shows the condition of craftsmanship execution structure of the FBMC modulator [14, 15]. The quantity of subcarriers is signified by N. The mth complex info image on the nth transporter is indicated by $d_{n,m}$. On the off chance that we express $d_{n,m}$ as,

$$d_{n,m} = a_{n,m} + j b_{n,m} \quad (4)$$

where $a_{n,m}$ and $b_{n,m}$ denote the genuine and nonexistent information terms, separately, at that point $a_{n,m}$ and $b_{n,m}$ are part and taken care of into upper and lower IDFTs with the stage move terms increased. The stage move term of then $a_{n,m}$ (at the nth component of upper IDFT input vector) is signified by $\eta_{n,m}$ and the stage move term of then $b_{n,m}$ (at the nth component of lower IDFT input vector) is indicated by $\mu_{n,m}$, as appeared in Fig. 2(a). To consent to the FBMC signal arrangement, $\eta_{n,m}$ and $\mu_{n,m}$ must fulfil the accompanying rule [14, 16]:

$$\eta_{n,m} = \begin{cases} 1 \text{ (or } -1) & \text{if } n = \text{even,} \\ j \text{ (or } -j) & \text{if } n = \text{odd,} \end{cases}$$

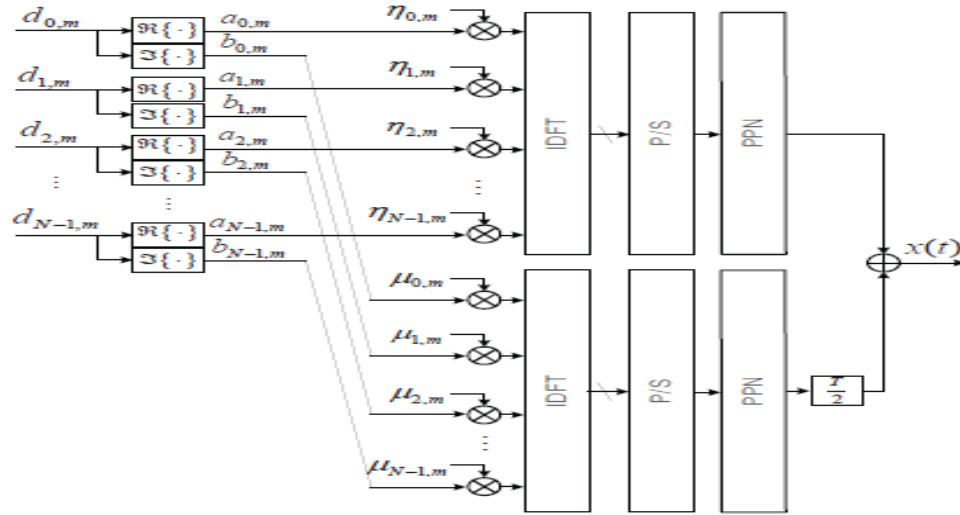
$$\mu_{n,m} = \begin{cases} j \text{ (or } -j) & \text{if } n = \text{even,} \\ 1 \text{ (or } -1) & \text{if } n = \text{odd.} \end{cases}$$

(5)

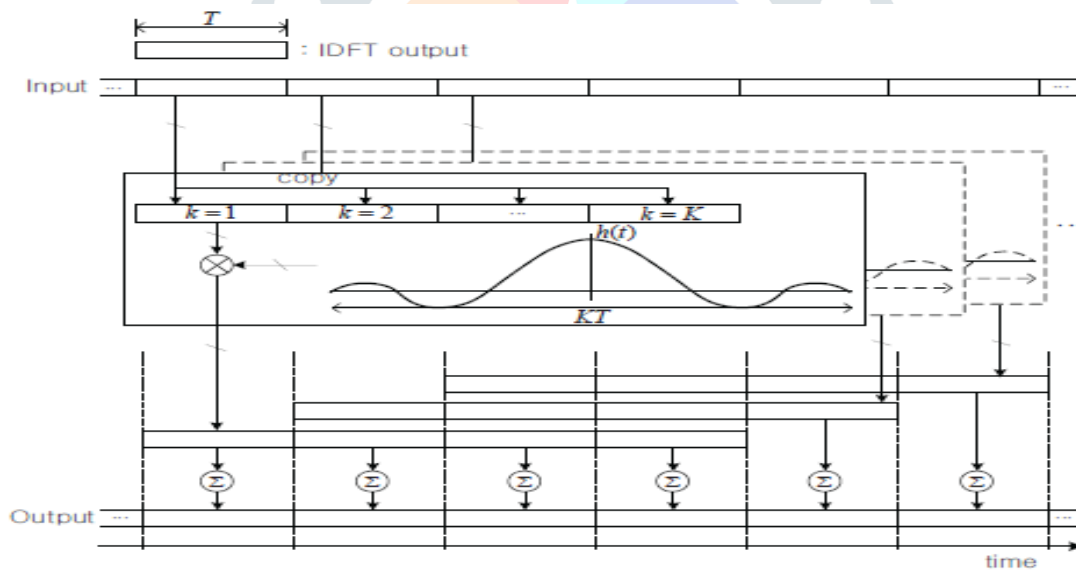
Utilizing the PPN (polyphase organization) method [14], the individual heartbeat moulding of each subcarrier can be performed immediately at the yield phase of IDFT, as appeared in Fig. 2(a). With the cover and-total technique [14, 15, 17], the PPN can be unequivocally executed as appeared in Fig. 2(b)

where T indicates the perplexing information image span of each subcarrier, $h(t)$ signifies the drive reaction of the beat forming model channel, and K means the covering variable of the beat. The activity of the PPN in Fig.2(b) is clarified as follows[15]: First, each IDFT yield vector is replicated K occasions and is reshaped. At that point, the inspected adaptation of $h(t)$ over K image term is increased to the reshaped IDFT yield vector. This is progressively performed for each IDFT yield vector

as outlined in stacked boxes of Fig. 2(b). At last, as appeared in the lower part of Fig. 2(b), every one of the duplicated vectors is lined up with its relating input (= IDFT yield) vector timing and afterward, is added together to create the yield succession of the PPN. To present 1/2 image timing counterbalance between IQ channels for OQAM, the yield of the lower PPN in Fig. 2(a) goes through $T/2$ -defer block.



(a) Implementation Structure of FBMC



(b) An explicit Implementation of PPN

Fig. 2. Implementation structure of FBMC and PPN.

In [11–13], enlivened by the SC-FDMA, the writers researched the DFT-spread FBMC as appeared in Fig. 2. In the DFT-spread FBMC in [11–13], the DFT-spread information vector is legitimately taken care of to the FBMC input. Let the perplexing

vector $[D_{n,m}]_{n=0}^{N-1} = ([A_{n,m} + jB_{n,m}]_{n=0}^{N-1})$ signify the DFT yield vector when the DFT input vector is the information image vector $[d_{n,m}]_{n=0}^{N-1} = ([a_{n,m} + jb_{n,m}]_{n=0}^{N-1})$ as appeared in Fig. 3

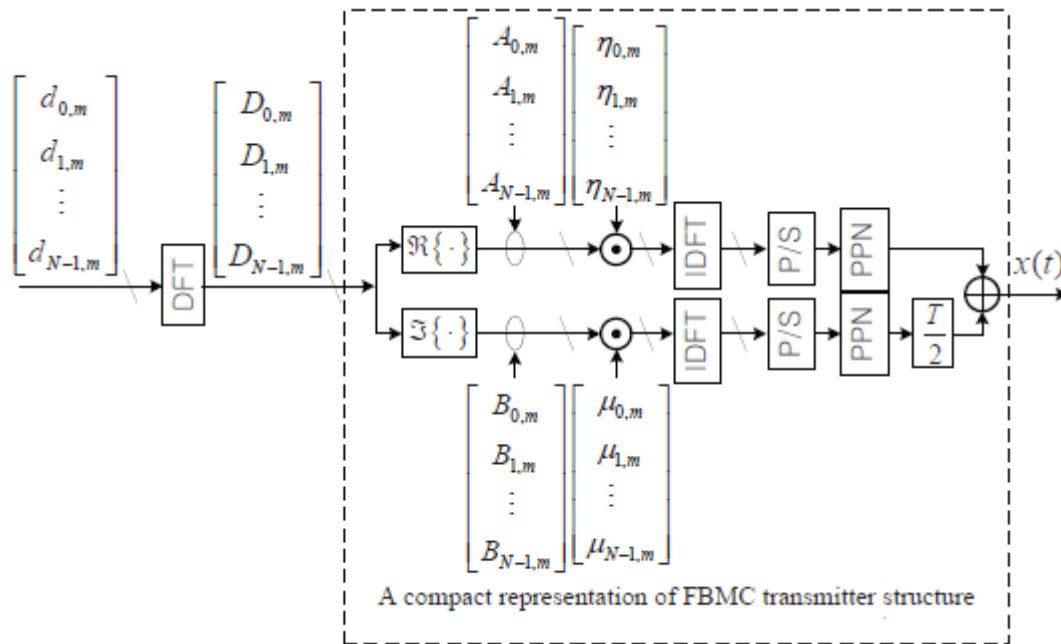


Fig.3. Implementation structure of DFT-spread FBMC, ⊙ denotes element-by- element multiplication.

A. Structure and algorithm of the proposed DFT-spread FBMC Transmitter and Receiver

The information outline is separated into successive squares, every one of which contains W FBMC images. With respect to second factor of the proposed PAPR decrease conspire referenced above, we create four adaptations of the DFT-spread and ITSM-moulded FBMC waveforms for every information block. Initial two variants for the *l*th information block meant by $x_l^{(1)}(t)$ and $x_l^{(2)}(t)$ are made equivalent and individually, with the image file *m* restricted to the *l*th information block, i.e., $lw \leq m \leq (l + 1)W - 1$ as follows:

$$x_l^{(1)}(t) = \sum_{n=0}^{N-1} \sum_{m=lw}^{(l+1)W-1} (-1)^m \{A_{n,m}h(t - mT) + jB_{n,m}h(t - mT - \frac{T}{2})\} e^{jn\frac{2\pi}{T}(t+\frac{T}{4})}$$

(6)

$$x_l^{(2)}(t) = \sum_{n=0}^{N-1} \sum_{m=lw}^{(l+1)W-1} (-1)^m \{A_{n,m}h(t - mT) + jB_{n,m}h(t - mT - \frac{T}{2})\} e^{jn\frac{2\pi}{T}(t-\frac{T}{4})}$$

(7)

Note that the subcarriers in (7) are simply T/2 time moved adaptations of those in (4.22). Accepting rectangular heartbeat moulding for straightforwardness, (6) and (7) in the IQ covered time frame FBMC image are the single transporter signals with time move T/4 and - T/4, separately.

Then again, in the outside of the covered span, each FBMC image covers with the back to back FBMC images, and consequently the distinctive time move in the multicarrier brings about very various waveforms. In this manner, the pinnacle forces of the two waveforms are likewise not the same as one another.

In (6) and (7), the Q channel is one-half image deferred for OQAM adjustment before multicarrier regulation. Regardless of whether the I channel rather than the Q channel is one-half image postponed, the FBMC signal configuration and the ITSM condition are as yet fulfilled. Henceforth, for the other two variants for the *l*th information block meant by $x_l^{(3)}(t)$ and $x_l^{(4)}(t)$, we consider the changed renditions of (6) and (7), separately, where the I channel is deferred rather than the Q channel, as follows:

$$x_l^{(3)}(t) = \sum_{n=0}^{N-1} \sum_{m=lw}^{(l+1)W-1} (-1)^m \{A_{n,m}h(t - mT - \frac{T}{2}) + jB_{n,m}h(t - mT)\} e^{jn\frac{2\pi}{T}(t+\frac{T}{4})}$$

(8)

$$x_l^{(4)}(t) = \sum_{n=0}^{N-1} \sum_{m=lw}^{(l+1)W-1} (-1)^m \{A_{n,m}h(t - mT - \frac{T}{2})$$

$$+ jB_{n,m}h(t - mT)\} e^{jn\frac{2\pi}{T}(t-\frac{T}{4})} \tag{9}$$

As the images in the IQ covered periods continue as before regardless of the postponement in I or Q channel, (8) and (9) are equivalent to (6) and (7), individually in the IQ covered stretch, accepting rectangular heartbeat for effortlessness. In any case, contingent upon which channel is postponed, the pinnacle forces of the two variants are extraordinary. The postponed channel image covers the ensuing OQAM image and the non-deferred channel image covers the former image. Along these lines, the pieces of the sign external the covered span are distinctive relying upon which channel is postponed and accordingly, the general waveforms of the two variants are unique. Summarizing, the pinnacle forces of the four waveforms in (6), (7), (8) and (9) are diverse one another and this propelled us to add an up-and-comer determination thought to the ITSM-adapted and DFT-spread FBMC.

$$x_l^{(3)}(t) = \sum_{n=0}^{N-1} \sum_{m=lW}^{(l+1)W-1} (-1)^m \{jA_{n,m}h(t - mT - \frac{T}{2}) - B_{n,m}h(t - mT)\} e^{jn\frac{2\pi}{T}(t+\frac{T}{4})} \tag{10}$$

$$x_l^{(4)}(t) = \sum_{n=0}^{N-1} \sum_{m=lW}^{(l+1)W-1} (-1)^m \{jA_{n,m}h(t - mT - \frac{T}{2}) - B_{n,m}h(t - mT)\} e^{jn\frac{2\pi}{T}(t-\frac{T}{4})} \tag{11}$$

In (10) and (11), j is duplicated to the postponed direct as in (6) and (7), and this permits the expansion of sequential information impedes independent of their ITSM condition forms. This change is actualized utilizing a contingent multiplier at the last phase of Fig. 4.4.

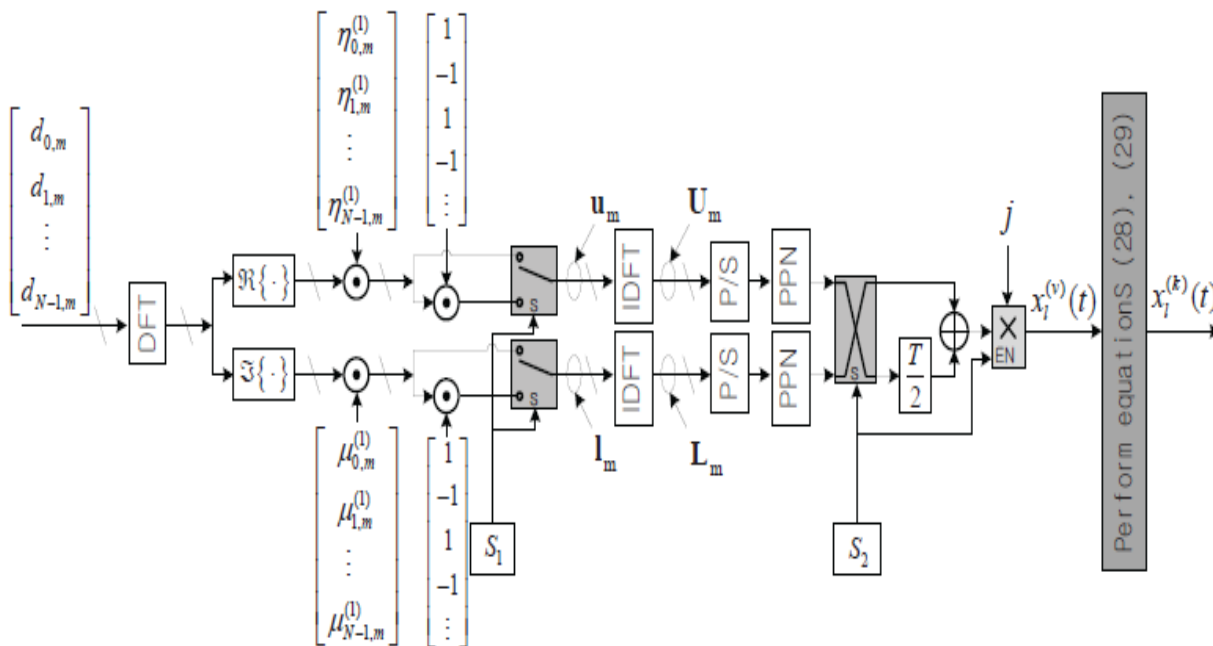


Fig .4. Transmitter of the proposed FBMC, ⊙ denotes element-by-element multiplication

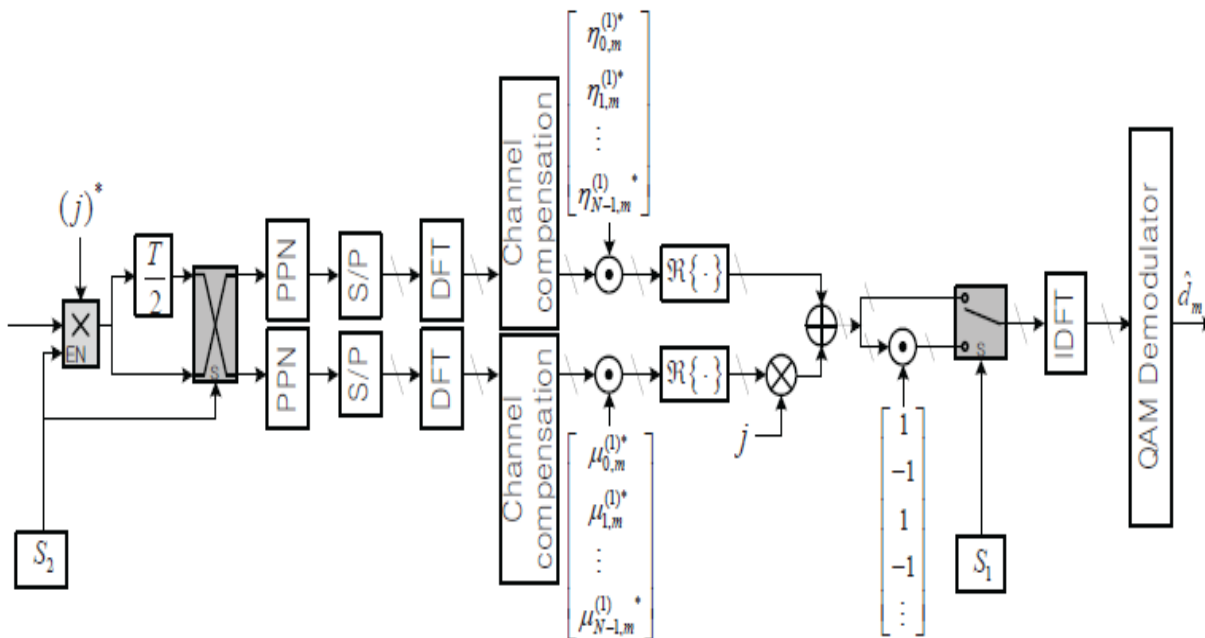


Fig .5. Receiver of the proposed FBMC, ⊙ denotes element-by-element multiplication.

4. SI-LP-FBMC

We propose a SI-installed LP-FBMC that doesn't independently send the SI yet inserts it in the communicated signal. SI is identified in such a visually impaired way with the assistance of the adjusted sign structure.

A. Constellation-invariant property of LP-FBMC, demodulated by incorrect ITSM versions

In this subsection, we show a unique natural property of LP-FBMC competitor waveforms: regardless of whether the LPFBMC signal is demodulated by an inaccurate ITSM variant, simply a half-vector trade or a 90-degree stage revolution happens in the information image vector, and subsequently the star grouping stays invariant. This property permits us to devise a SI-inserted signal structure.

For a manageable investigation, we follow the essential supposition of semi static blurring over the nearby subcarriers and the successive images in the range of the utilized range forming beat h(t). To disengage the components that are insignificant to the verification of the heavenly body invariant property, we expect there is no noise and wonderful channel remuneration. The assessment of $A_{k,i}$ in (5) and the assessment of $B_{k,i}$ are then composed as:

$$\begin{aligned} \hat{A}_{k,i} &= \Re \left[\int_{-\infty}^{\infty} x_l^{(c)}(t) \{p_{k,i}^{(\hat{c})}(t)\}^* dt \right] \\ \hat{B}_{k,i} &= \Re \left[\int_{-\infty}^{\infty} x_l^{(c)}(t) \{q_{k,i}^{(\hat{c})}(t)\}^* dt \right] \end{aligned} \tag{12}$$

Let us consider a situation when the lth information subframe is demodulated in the way of the fixed ITSM variant, paying little heed to the real ITSM rendition. For simplicity of clarification, we consider a situation when the signal is demodulated in the way of the primary ITSM variant; i.e., \hat{c} in (12) is compelled to be 1, paying little mind to c. We signify the factors variables $\hat{A}_{k,i}$, $\hat{B}_{k,i}$, $D_{k,i}$ and $\hat{d}_{k,i}$ for this constrained case as $\tilde{A}_{k,i}$, $\tilde{B}_{k,i}$, $\tilde{D}_{k,i}$ and $\tilde{d}_{k,i}$ individually as follows:

$$\begin{aligned} \tilde{A}_{k,i} &\triangleq \Re \left[\int_{-\infty}^{\infty} x_l^{(c)}(t) \{p_{k,i}^{(1)}(t)\}^* dt \right] \\ \tilde{B}_{k,i} &\triangleq \Re \left[\int_{-\infty}^{\infty} x_l^{(c)}(t) \{q_{k,i}^{(1)}(t)\}^* dt \right] \end{aligned} \tag{13}$$

$$\tilde{D}_{k,i} \triangleq \tilde{A}_{k,i} + j\tilde{B}_{k,i} \tag{14}$$

$$[\tilde{d}_{k,i}]_{k=0}^{N-1} \triangleq \text{IDFT} \left[[\tilde{D}_{k,i}]_{k=0}^{N-1} \right] \tag{15}$$

For the correct ITSM version (i.e., when $c=1$ in (13)), the demodulated data symbol vector should be correct as follows:

$$[\tilde{d}_{k,i}]_{k=0}^{N-1} = [d_{k,i}]_{k=0}^{N-1} \tag{16}$$

B. Embedding SI by rotated constellation

The four ITSM variants of LP-FBMC have indistinguishable groups of stars, with demodulation even by an off base ITSM adaptation. This roused a basic thought of installing the SI utilizing diversely pivoted groups of stars for the distinctive ITSM

variants. At that point, in the recipient, we recognize the SI by estimating the stage revolution of the group of stars kept up all through each subframe. In Fig. 6, we present the one-half image timing counterbalance between IQ branches in the FBMC regulation stage as the regular FBMC-OQAM. The terms QAM and quadrature phase-shift keying (QPSK) are utilized to allude to the group of stars for the information image before the DFT spreading stage in Fig.6. Subsequently, the prefix "O" which means Offset and should be overlooked in these terms.

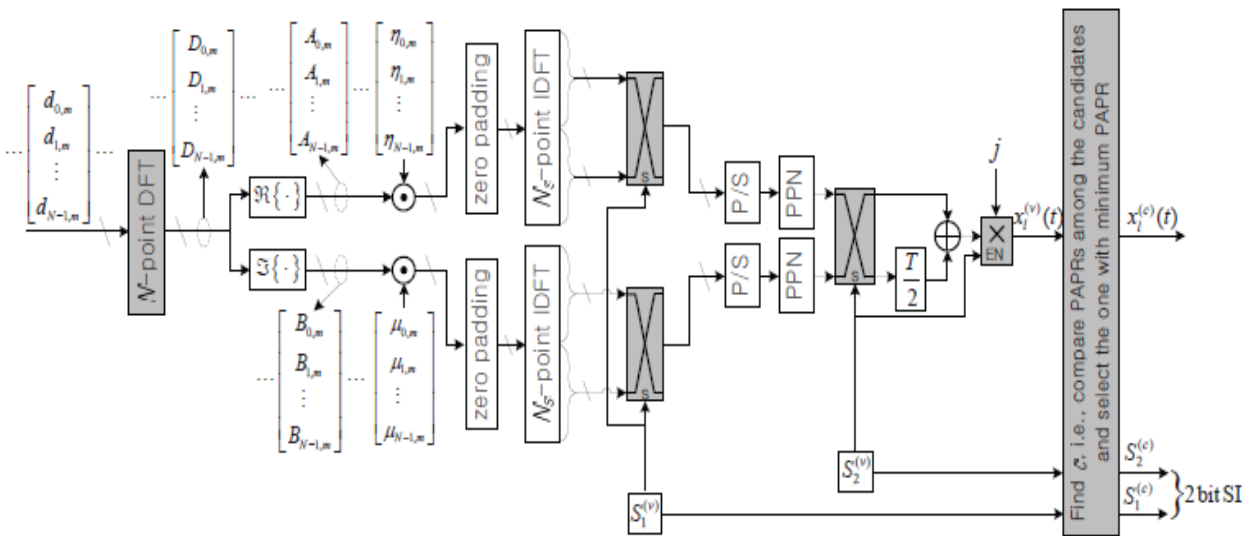


Fig 6 Structure of the SI-embedded LP-FBMC receiver

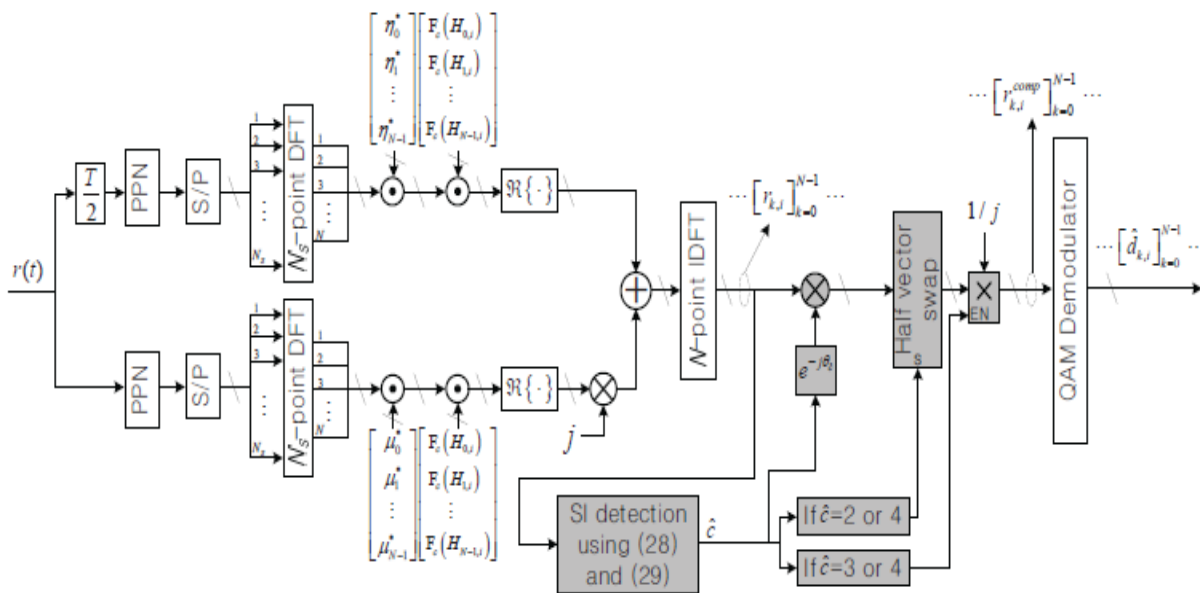
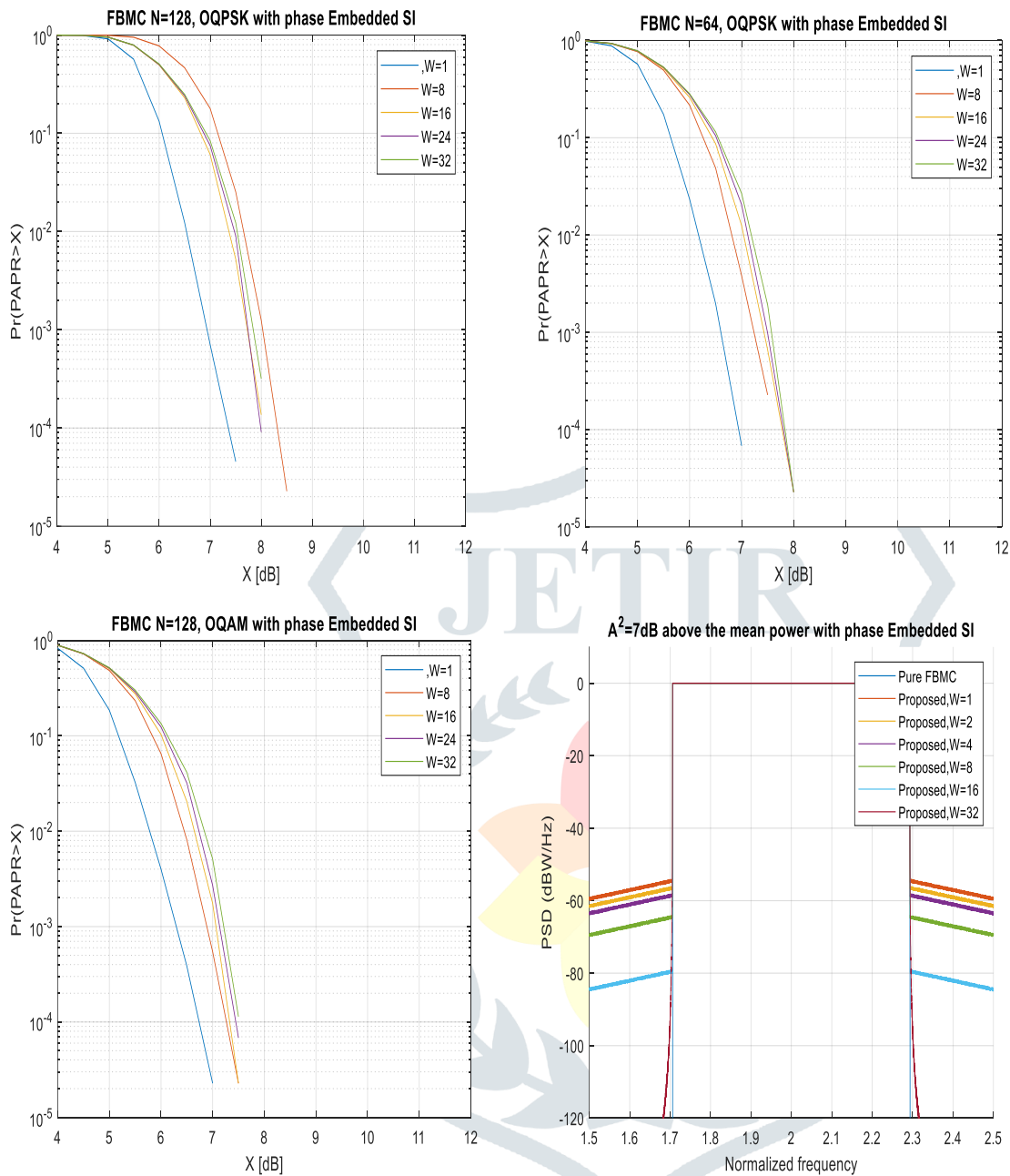
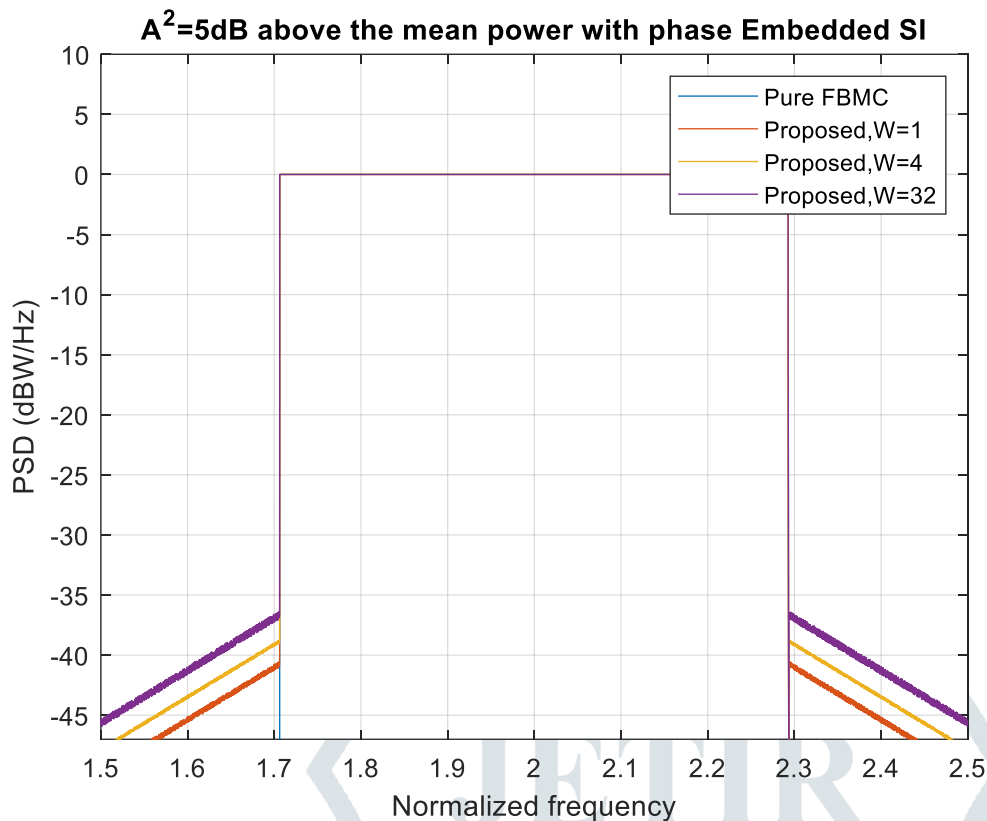


Fig 7. Structure of the SI-embedded LP-FBMC receiver

5. Results and Discussion





6. Conclusion

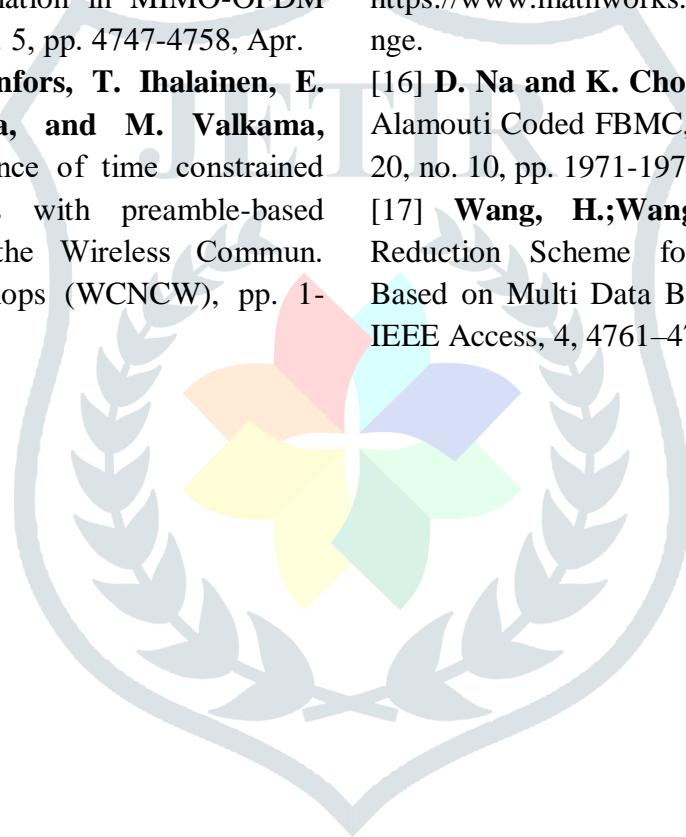
In this paper, we proposed a low PAPR FBMC plot and affirmed its exceptional execution contrasted with the current PAPR decrease plans regarding PAPR decrease gain, calculation unpredictability overhead and SI overhead. We previously inferred the supposed ITSM (indistinguishably time-moved multicarrier) condition, which completely misuses the single transporter impact of DFT spread FBMC. At that point, to additional improve the measure of PAPR decrease, we produce the four up-and-comer renditions of the DFT-spread and ITSM-adapted FBMC waveform and select the one

with least pinnacle power. Utilizing the proposed plot, we settled a forthcoming issue of FBMC, i.e., OOB range re-development because of HPA nonlinearity. We indicated that even with the HPA nonlinearity, the proposed conspire significantly stifles the OOB range re-development and still accomplishes the best range confinement among the plans in correlation. Further we considered stage inserted side data and the outcomes are gotten. By the cycle inserting the data the PAPR is diminished as appeared in outcomes

References

- [1] **B. Farhang-Boroujeny, (2011).** "OFDM versus filter bank multicarrier," IEEE Sig. Proc. Mag., vol. 28, no. 3, pp. 92-112, May.
- [2] **M. Renfors, X. Mestre, E. Kofidis, and F. Bader, (2017).** Eds, Orthogonal Waveforms and Filter Banks for Future Communication Systems, Academic Press.
- [3] **R. Nissel, S. Schwarz, and M. Rupp, (2017).** "Filter bank multicarrier modulation schemes for future mobile communications," IEEE J. Sel. Areas Commun., vol. 35, no. 8, pp. 1768-1781, Aug.
- [4] **C. L'el'e, J.-P. Javaudin, R. Legouable, A. Skrzypczak, and P. Siohan, (2008).** "Channel estimation methods for preamble-based OFDM/OQAM modulations," European Trans. Telecommun., no. 19, no. 7, pp. 741-750, Nov.
- [5] **C. L'el'e, P. Siohan, and R. Legouable, (2008).** "2 dB better than CP-OFDM with OFDM/OQAM for preamble-based channel estimation," in Proc. Int. Conf. Commun., pp. 1302-1306, Beijing, China, May.
- [6] **J. Du and S. Signell, (2009).** "Novel preamble-based channel estimation for OFDM/OQAM," in Proc. Int. Conf. Commun., pp. 14-18, Dresden, Germany, Jun.

- [7] **S. Hu, G. Wu, T. Li, Y. Xiao, and S. Li, (2010).** "Preamble design with ICI cancellation for channel estimation in OFDM/OQAM system," IEICE Trans. Commun., E93-B, pp. 211-214, Jan.
- [8] **E. Kofidis, D. Katselis, A. Rontogiannis, and S. Theodoridis, (2013).** "Preamble-based channel estimation in OFDM/OQAM systems: A review," Signal Process., vol. 93, no. 7, pp. 2038-2054, Jul.
- [9] **S. Taheri, M. Ghoraishi, and P. Xiao,(2015).** "Overhead reduced preamble-based channel estimation for MIMO-FBMC systems," in the Int. Wireless Commun. Mobile Comput. Conf. (IWCMC), Dubrovnik, Croatia, Aug. pp. 1435-1439.
- [10] **S. Hu, Z. Liu, Y. L. Guan, C. Jin, Y. Huang, and J.-M. Wu, (2017).** "Training sequence design for efficient channel estimation in MIMO-OFDM systems," IEEE Access, vol. 5, pp. 4747-4758, Apr.
- [11] **T. Levanen, M. Renfors, T. Ihalainen, E. Lahetkangas, V. Syrjala, and M. Valkama, (2016).** "On the performance of time constrained OQAMOFDM waveforms with preamble-based channel estimation," in the Wireless Commun. Networking Conf. Workshops (WCNCW), pp. 1-7, Doha, Qatar, Apr.
- [12] **A. Viholainen, M. Bellanger, and M. Huchard, (2009).** "PHYDAS-PHYSical layer for Dynamic Access and cognitive radio Report D5.1," Available: [www.ict-phydyas.org / delivrables / PHYDYAS-D5-1.pdf](http://www.ict-phydyas.org/delivrables/PHYDYAS-D5-1.pdf), 2009.
- [13] **C. H. Yuen, P. Amini, and B. Farhang-Boroujeny, (2010).** "Single carrier frequency division multiple access (SC-FDMA) for filter bank multicarrier communication systems," in Proc. CROWNCOM, pp. 1-5, June. 2010.
- [14] **M. Bellanger, D. L. Ruyet, D. Roviras, and M. Terre, (2010).** "FBMC physical layer: a primer," PHYDYAS FP7 Project Document, Jan.
- [15] **M. Terre, "FBMC Modulation / Demodulation,"** MATLAB Central Available: <https://www.mathworks.com/matlabcentral/fileexchange>.
- [16] **D. Na and K. Choi, (2016).** "Intrinsic ICI-Free Alamouti Coded FBMC," IEEE Commun. Lett., vol. 20, no. 10, pp. 1971-1974, Oct.
- [17] **Wang, H.;Wang, (2016).** Hybrid PAPR Reduction Scheme for FBMC/OQAM Systems Based on Multi Data Block PTS and TR Methods. IEEE Access, 4, 4761–4768.



ABOUT THE AUTHOR

B. PRAVALIKA is a post graduate student in the department of systems and signal processing (ECE) at JNTUK-University college of Engineering Vizianagaram, Andhra Pradesh, India. She is completed her B. Tech degree in the department of Electronics and Communication Engineering, JNTU- Kakinada, Andhra Pradesh, India.



R. GURUNADHA is currently working as an assistant Professor at the Department of Electronics and Communication Engineering at University College of Engineering Vizianagaram, JNTUK, India. He completed his B.E from Andhra University, India and M.Tech from JNTU Hyderabad, India. His areas of interest are VLSI, Signal Processing and Embedded systems.

